Title	An experimental and modeling study of surrogate mixtures of n-propyl- and n-butylbenzene in n-heptane to simulate n-decylbenzene ignition
Author(s)	Darcy, D,Nakamura, H,Tobin, CJ,Mehl, M,Metcalfe, WK,Pitz, WJ,Westbrook, CK,Curran, HJ; Darcy, Daniel; Nakamura, Hisashi; Tobin, Colin J.; Mehl, Marco; Metcalfe, Wayne K.; Pitz, William J.; Westbrook, Charles K.; Curran, Henry J.
Publication Date	2014-01-11
Publication Information	Darcy, D,Nakamura, H,Tobin, CJ,Mehl, M,Metcalfe, WK,Pitz, WJ,Westbrook, CK,Curran, HJ (2014) 'An experimental and modeling study of surrogate mixtures of n-propyl- and n-butylbenzene in n-heptane to simulate n-decylbenzene ignition'. Combustion And Flame, 161 :1460-1473.
Publisher	Elsevier ScienceDirect
Link to publisher's version	http://dx.doi.org/10.1016/j.combustflame.2013.12.006
Item record	http://hdl.handle.net/10379/6125
DOI	http://dx.doi.org/10.1016/j.combustflame.2013.12.006

An experimental and modeling study of surrogate mixtures of *n*-propyl- and *n*-butylbenzene in *n*-heptane to simulate *n*-decylbenzene ignition

D. Darcy[a], H. Nakamura[a,b], C.J. Tobin[a], M. Mehl[c], W.K. Metcalfe[a], W.J. Pitz[c], C.K. Westbrook[c], H.J. Curran[a,*]

[a]*Combustion Chemistry Centre, NUI Galway, Ireland*
[b]*Institute of Fluid Science, Tohoku University, 2-1-1 Katahira, Aoba-ku, Sendai, Miyagi 980-8577 Japan*
[c]*Lawrence Livermore National Laboratory, Livermore, CA 94551*

Abstract

This paper presents experimental data for the oxidation of two surrogates for the large alkylbenzene class of compounds contained in diesel fuels, namely *n*-decylbenzene. A 57:43 molar % mixture of *n*-propylbenzene:*n*-heptane in air ($\approx$21% O_2, $\approx$79% N_2) was used in addition to a 64:36 molar % mixture of *n*-butylbenzene:36% *n*-heptane in air. These mixtures were designed to contain a similar carbon/hydrogen ratio, molecular weight and aromatic/alkane ratio when compared to *n*-decylbenzene. Nominal equivalence ratios of 0.3, 0.5, 1.0 and 2.0 were used. Ignition times were measured at 1 atm in the shock tube and at pressures of 10, 30 and 50 atm in both the shock tube and in the rapid compression machine. The temperature range studied was from approximately 650–1700 K. The effects of reflected shock pressure and equivalence ratio on ignition delay

*address: Combustion Chemistry Centre, School of Chemistry, NUI Galway, Ireland. Phone: 00353-91-493856. Email: henry.curran@nuigalway.ie
  URL: http://c3.nuigalway.ie/ (H.J. Curran)

time were determined and common trends highlighted. It was noted that both mixtures showed similar reactivity throughout the temperature range studied. A reaction mechanism published previously was used to simulate this data. Overall the reaction mechanism captures the experimental data reasonably successfully with a variation of approximately a factor of 2 for mixtures at 10 atm and fuel-rich and stoichiometric conditions.

1. Introduction

To ensure remaining transport fuel supplies are efficiently consumed along with the minimization of emissions from these fuels, it is important to fully understand the chemistry of them. Unfortunately market fuels are complex mixtures of hydrocarbon components and as such to examine the chemistry behind each component is impractical. For this reason surrogate mixtures have been devised to represent fuels while only containing components representative of each class present in the fuel [1–3]. Farrell *et al.* [1] identified *n*-decylbenzene as a possible fuel surrogate component to represent the aromatic class in diesel fuel. To use *n*-decylbenzene as a component in a diesel surrogate fuel, a detailed chemical kinetic mechanism needs to be developed and experimental data for its validation needs to be obtained. Unfortunately, it is difficult to study *n*-decylbenzene in shock tubes and rapid compression machines (RCM) due to its extremely low vapor pressure. To circumvent this issue, we propose to create a series of surrogates for *n*-decylbenzene using mixtures of *n*-propylbenzene and *n*-heptane and *n*-butylbenzene and *n*-heptane whose vapor pressures are adequate for the investigations used in this study. The *n*-heptane and the alkyl side chain on *n*-propylbenzene and *n*-butylbenzene would mimic the *n*-decyl side chain on *n*-decylbenzene and provide a fuel surrogate mixture that simulates the chemical properties of a large alkyl benzene. In this study we chose a mixture of 43:57% *n*-heptane:*n*-propylbenzene and 36:64% *n*-heptane:*n*-butylbenzene by mole. These mixtures were chosen to have a similar hydrogen:carbon ratio (1.685 and 1.65) content when compared to *n*-decylbenzene whose hydrogen:carbon ratio is 1.625.

3

We have used two separate surrogates for the same fuel to investigate the impact that the additional methyl group of *n*-butylbenzene has on the reactivity when mixed with *n*-heptane.

A number of studies have been performed on the single component fuels *n*-propylbenzene, *n*-butylbenzene and *n*-heptane. We first review the *n*-propylbenzene studies. Litzinger *et al.* used a plug-flow reactor to study its oxidation at 1 atm pressure, at a temperature of approximately 1060 K and at equivalence ratios of 0.65, 1.0 and 1.5 highly diluted in nitrogen (99%) [4].

Roubaud *et al.* carried out rapid compression machine experiments on eleven different alkylbenzenes (including *n*-propylbenzene) in the lower temperature region (600–900 K), at compressed pressures of up to 25 bar for stoichiometric mixtures in air [5, 6].

Dagaut *et al.* [7] carried out experiments in a jet-stirred reactor (JSR) on *n*-propylbenzene oxidation at atmospheric pressure over a temperature range of 900–1250 K at atmospheric pressure and at equivalence ratios of 0.5, 1.0 and 1.5 highly diluted in nitrogen (≥ 50 ppm of O_2 and H_2O; ≥ 1000 ppm of Ar; ≥ 5 ppm of H_2). These experiments provided concentration versus temperature profiles of 23 different species. In addition, they developed a kinetic reaction mechanism for the oxidation of *n*-propylbenzene containing 124 species and 985 reactions.

A recent study by Gudiyella and Brezinsky [8] on *n*-propylbenzene produced high-pressure single-pulse shock tube speciation data obtained at shock pressures of 25 and 50 atm, at temperatures between 838–1669 K and equivalence ratios between 0.5–1.9. Species concentration versus temperature data for a variety of

stable species was reported. A kinetic model has also been reported in this study.

Darcy *et al.* [9] measured ignition delay times in a heated high pressure shock tube for mixtures of *n*-propylbenzene in air at equivalence ratios of 0.29, 0.48, 0.96 and 1.92 and at reflected shock pressures of 1, 10 and 30 atm in the intermediate-to high-temperature regime (1000–1600 K). A comparative study with *n*-butylbenzene was also performed at these conditions, with both alkyl benzenes showing very similar reactivity. Moreover, a detailed chemical kinetic mechanism was used to simulate this data. This mechanism was based on that published for *n*-propylbenzene oxidation and subsequently modified for *n*-butylbenzene oxidation in a jet-stirred reactor at 10 atm under dilute conditions over the temperature range 550–1180 K and at equivalence ratios of 0.25, 0.5, 1.0 and 2.0 by Diévart and Dagaut [10]. This study was further extended to include lower temperature experiments in a subsequent publication [11]. Model predictions and experimental data showed very good agreement in both the high and low temperature regime.

Next we review the *n*-butylbenzene literature studies. These are even fewer than those of *n*-propylbenzene. In the Roubaud *et al.* [5, 6] study, *n*-butylbenzene was another of the alkylbenzenes studied in the rapid compression machine at temperatures of 600–900 K at compressed pressures of up to 25 bar for stoichiometric mixtures in air. According to Roubaud et al. [5] alkylbenzenes can be divided into two groups according to their autoignition characteristics. The compounds in the first group present features of low-temperature reactivity such as a negative temperature coefficient (NTC) zone: o-xylene, 1,2,3-trimethylbenzene and *n*-butylbenzene. A mechanism was proposed by Ribaucour et al. [12] to sim-

ulate the autoignition of *n*-butylbenzene in a rapid compression machine. The oxidation of *n*-butylbenzene has recently been studied in a jet-stirred reactor [10] in the temperature range 550–1150 K, at 10 bar, for equivalence ratios from 0.25 to 1.5, and at a residence time of 1 s. In these experiments, only very low reactivity was observed below 800 K, even for the leanest mixtures, because of the very large dilution (0.1% initial fuel mole fraction) used in this study. These results have been simulated [10] using a model based on that of Ribaucour et al. [12].

A recent study on *n*-butylbenzene oxidation was carried out by Husson *et al.* [13] in which experimental data was obtained in a variety of experimental facilities including a shock tube, rapid compression machine and a jet stirred reactor over the temperature range of 640–1740 K at pressures between 1 and 30 atm and equivalence ratios between 0.25 and 2.0. This study simulated these data using a reaction mechanism including 393 species and 2303 reactions produced for the paper which shows good agreement between experiments and simulations.

Nakamura et al [14] carried out a study on *n*-butylbenzene in a rapid compression machine and high pressure shock tube at equivalence ratios of 0.3, 0.5, 1.0 and 2.0 at pressures of 1, 10, 30 and 50 atm over a wide temperature range (700–1700 K) and compared this data with our reaction mechanism [11]. The data and mechanism simulations showed good agreement for most conditions studied with some discrepancies at low temperatures.

With respect to studies on *n*-heptane, its ignition behavior has been investigated extensively as a primary reference fuel and as part of a surrogate fuel mixture to represent larger fuels in both experimental [15–45] and modeling stud-

6

ies [46–54]. Due to the volume of studies on *n*-heptane we will focus our attention to those studies in which *n*-heptane has been added to aromatic compounds to measure auto-ignition. In particular the auto-ignition of mixtures of *n*-heptane and toluene have been extensively studied in shock tubes [16, 18], test engines [55–61], and RCM's [62–64]. Of particular interest was the study of Herzler *et al.* [16] in which a mixture of 65% toluene and 35% *n*-heptane was studied in a shock tube. When this data was compared to that of pure *n*-heptane, reduced NTC reactivity was observed. This observation was further supported in the study of Hartmann *et al.* [18] who noted, while studying toluene / *n*-heptane blends containing up to 40% toluene, that above 20% toluene any further addition of toluene inhibited reactivity and resulted in reduced NTC reactivity.

Previously we have published shock tube data for the *n*-propylbenzene / *n*-heptane mixtures of this study [65]. This study aims to extend this data into the low temperature regime while also comparing the entire temperature range with the *n*-butylbenzene /*n*-heptane mixtures. Nominal equivalence ratios of 0.3, 0.5, 1.0 and 2.0 were used for *n*-propylbenzene / *n*-heptane mixtures. For both mixtures compressed pressures of 10, 30 and 50 atm were measured while the temperature range studied was from approximately 650–1700 K. Experimental data for 1 atm is provided at high temperature and an equivalence ratio of 0.5, 1.0, and 2.0.

Overall this study examines the key trends observed in mixtures of *n*-propylbenzene and *n*-heptane, *n*-butylbenzene and *n*-heptane and will also show a comparison between both surrogates. Also investigated was the effect of mixing *n*-

7

propylbenzene and *n*-heptane when compared to pure *n*-propylbenzene and pure *n*-heptane, in this case a representative condition of $\phi = 1.0$ at 10 atm pressure was chosen.

2. Experimental

2.1. Shock tube

Shock tube experimental data was measured in the NUI Galway High Pressure Shock Tube. This shock tube has been described when the *n*-propylbenzene shock tube data was first published [65]. This shock tube consists of a stainless steel tube of 8.76 m in length, with an internal diameter of 6.3 cm. A double-diaphragm section divides the shock tube into a 3 m long driver section and a 5.73 m driven section. Polyethylene terephthalate films (KATCO) or aluminium plates were used as diaphragms in all experiments, where the thickness of the diaphragm material was chosen depending on the desired final shock pressure and varied from 75–500 μm for the polyethylene terephthalate films and 0.8–2.0 mm for the aluminium plates. The driver gas used was helium (99.99% pure; BOC). The operational pressure limit of the shock tube is approximately 60 bar. The diagnostic system involves four pressure transducers, where the velocity of the incident shock wave was measured at three locations separated by known distances with the shock velocity extrapolated to the endwall. The pressure at the endwall was monitored using a pressure transducer (PCB, 113A24). The incident shock velocity at the endwall was used to calculate the temperature and pressure of the mixtures behind the reflected shock wave using the equilibrium program

8

Gaseq [66].

The ignition delay time was defined as the interval between the rise in pressure due to the arrival of the shock wave at the endwall and the maximum rate of rise of the pressure signal. Pressure traces were obtained using a Sigma digital oscilloscope (Sigma, 90–4). Any experiments exhibiting significant pre-ignition pressure rise ($\geq$5% / ms) were excluded from the study in an attempt to minimize any non-ideal effects, in order for the data to be accurately simulated by assuming constant volume and homogeneous adiabatic conditions behind the reflected shock wave. Sample pressure/time profiles for similar mixtures have been presented in previous publications [9, 11, 65]. The initial temperature was varied from 363 to 403 K depending on the mixture composition, and was highest for the richest mixtures performed at the highest pressures.

Estimated uncertainty limits of the measurements are 1% in reflected shock temperature, T_5, $\pm$ 15% in ignition delay time, τ, and $\pm$ 2 % in mixture composition. All experimental data is provided as Supplementary Material.

2.2. Rapid compression machine

A rapid compression machine (RCM) is a laboratory device that simulates the compression stroke of a single engine cycle and allows auto-ignition phenomena to be studied in a more ideal, constant, and controllable environment than present in a reciprocating engine. Essentially an RCM raises the test gas to a high temperature and pressure as rapidly as possible while minimizing heat losses. The RCM used in *this study* is a clone of the original NUI Galway RCM which is

characteristically different to most other RCM's by having a twin-opposed piston configuration as described previously [67], resulting in a fast compression time of 15.7 ms. Creviced piston heads are additionally used to improve the post compression temperature distribution in the combustion chamber [68]. The design was for these creviced piston heads was originally devised at MIT [69, 70], but a computational fluid dynamics (CFD) study carried out at NUI Galway [71] suggested an improved crevice design which resulted in an almost homogeneous temperature field in the post compression period and found that the temperature field obtained using flat piston heads is far less homogeneous. The compression time was approximately 15.7 ms.

It was possible to use different sized piston heads to alter the compression ratio. The piston heads used in this study were high compression ratio heads with an approximate compression ratio of 13:1 and low compression ratio heads with an approximate compression ratio of 9.5:1. The compressed gas temperature was varied by using different proportions of Ar and N_2 in the diluent mixture, effectively varying the heat capacity of the fuel:diluent mixture. Using pure N_2 as diluent allows lower temperatures to be accessed, while the use of Ar allows higher temperatures to be studied due to the lower heat capacity of Ar compared to N_2. To avoid condensation of fuel components, the reaction chamber was wrapped in double-stranded heating tape (Flexelec, 1250 W) which was insulated by a single layer of insulation tape (Zetex 1000) allowing variation of the initial temperature up to a maximum operating temperature of 400 K. Sufficient time was allowed for the chamber temperature to stabilize after a change was made to the thermostat

10

setting.

Pressure-time profiles were measured using a pressure transducer (Kistler 603B) and transferred via an amplifier (Kistler 5018) to the oscilloscope (Picoscope 4424, USB PC oscilloscope) and ultimately recorded digitally on computer using the Picolog PC software. The ignition delay time, defined as the time from the peak pressure near the end of compression to the maximum rate of pressure rise during ignition, was measured using two vertical cursors on the oscilloscope. In general, it was found that the ignition delay times were reproducible to within 10% of one other at each compressed temperature. The compressed gas pressure was measured using two horizontal cursors. The primary experimental data comprised the pressure-time record, but it was more practical to assimilate and present the results in terms of the overall dependence of ignition delay on the compressed gas temperature.

The compressed gas temperature, T_C, was calculated using the initial temperature, T_i, pressure, p_i and reactant composition and the experimentally measured compressed gas pressure, p_C, defined as the maximum pressure immediately after compression, and employing the adiabatic compression/expansion routine in Gaseq [66], which uses the temperature dependence of the ratio of specific heats, γ, according to the equation:

$$\ln\left(\frac{p_c}{p_i}\right) = \int_{T_i}^{T_C} \frac{\gamma}{\gamma - 1} \frac{dT}{T}$$

while assuming frozen chemistry during compression. The compressed gas tem-

perature is then plotted against the measured ignition delay time to obtain over-all reactivity profiles of *n*-propylbenzene/*n*-heptane and *n*-butylbenzene/*n*-heptane mixtures.

Gases used, nitrogen (CP Grade) 99.95%, argon (Research Grade) 99.9995%, oxygen (Medical Grade) 99.5%, were supplied by BOC Ireland and were used without further purification. *n*-Propylbenzene, *n*-butylbenzene and *n*-heptane were obtained from Tokyo Chemicals Ltd at 99% purity (GC grade) and used without further purification.

Compression was achieved by simultaneous movement of the twin opposed pistons. The pressure-time history was recorded during and after compression until autoignition occurred.

The time for compression is fast, 15.7 ms, with most of the rapid rise in pressure and temperature taking place in the last 2-3 ms of compression; therefore heat losses during compression are low but do exist. For a period following compression the gases experience a high degree of heat loss owing to the swirl experienced and the high temperature of the gas within the chamber. Heat losses continue from the core gas after the end of compression. Even though ignition delays were observed up to 400 ms following compression, repeat experiments with ignition delay times greater than 100 ms showed larger percentage variations in measured ignition delay times than those with ignition delay times below 100 ms.

Estimated uncertainty limits of the measurements are $\pm$ 5 K in compressed gas temperature, $\pm$ 0.1 bar in compressed gas pressure, $\pm$ 15% in ignition delay time, τ, and $\pm$ 2 % in mixture composition. All experimental data is provided as

12

Supplementary Material.

2.3. Mixture preparation

As all fuels studied are liquids at room temperature mixtures were prepared by a direct injection method. In this method the fuel was injected via an injection port on the top of the heated mixing tanks using a gas-tight syringe (SGE Analytical Science, 5ml volume, 008760). The determined amount of fuel was added based on its weight measured using a scale (Ohaus, model: Adventurer Pro AV213C, to 3 decimal places) and the partial pressure of fuel was measured using an MKS pressure transducer and digital readout followed by the addition of oxygen and nitrogen to ensure the entire mixture composed the desired final pressure. Molar compositions of mixtures for both surrogates are shown in Tables 1 and 2.

Table 1: Molar composition of surrogate mixtures using n-propylbenzene

ϕ	% n-propylbenzene	% n-heptane	O_2	% Diluent
0.29	0.30	0.23	20.89	78.61
0.49	0.50	0.38	20.83	78.34
0.98	0.99	0.75	20.65	77.70
1.95	1.95	1.47	20.28	76.30

Table 2: Molar composition of surrogate mixtures using n-butylbenzene

ϕ	% n-butylbenzene	% n-heptane	O_2	% Diluent
0.3	0.32	0.18	20.89	78.61
0.5	0.53	0.30	20.83	78.35
1.0	1.05	0.59	20.66	77.70
2.0	2.07	1.16	20.32	76.45

The mixtures were left for approximately 1 hour before use to ensure homogeneity. Before an experiment in either facility the gas mixture was introduced
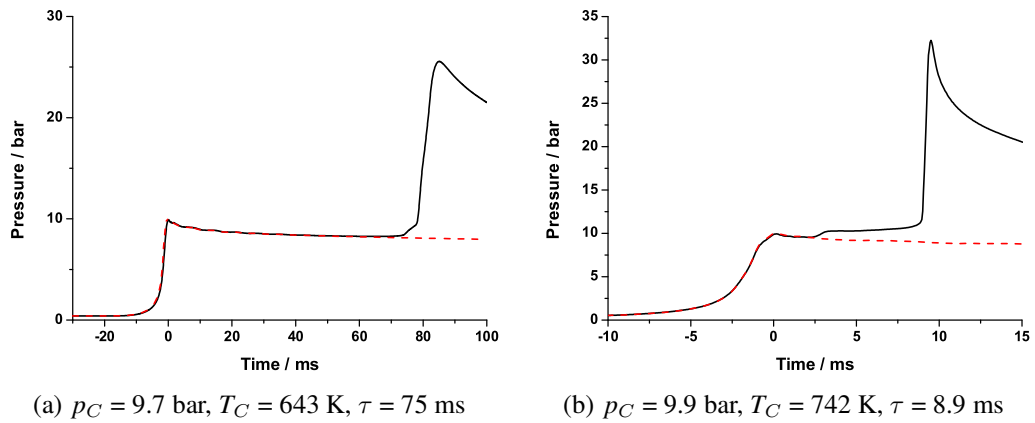
13

(a) $p_C = 9.7$ bar, $T_C = 643$ K, $\tau = 75$ ms (b) $p_C = 9.9$ bar, $T_C = 742$ K, $\tau = 8.9$ ms

Figure 1: Typical RCM pressure traces for 2.07% n-butylbenzene / 1.16% n-heptane, 20.32% O_2, $\phi = 2.0$. Solid line represents the reactive mixture while the dashed line represents the non-reactive mixture.

into the pre-heated compression cylinder from the mixing tank at a known temperature and pressure. Mixture compositions were verified by in-situ testing using an infra-red laser system similar to that of Mével *et al.* [72] who studied gas phase absorption cross sections at 3.39 μm to determine the concentration of twenty-one liquid hydrocarbons in the temperature range 303–413 K using an infrared He–Ne laser. Estimated uncertainties in our laser absorption measurements are 0.1 mbar in pressure, $\pm 1 - 2$ K in temperature and 0.2 mm in path length, with a total uncertainty of $\approx$ 2% in measured fuel concentration.

Typical pressure traces obtained in the rapid compression machine experiments are shown in Fig. 1. The reactive pressure trace is represented by the solid line while the non-reactive trace is depicted by the red dashed line.

14

3. Results

3.1. Chemical Kinetic Model

The chemical kinetic mechanism used to simulate this data has been discussed previously [11]. This mechanism was derived from the mechanism of Diévart and Dagaut [10] which was modified to include the latest C_0–C_4 base chemistry, pressure dependent rates for the unimolecular decomposition of both *n*-propylbenzene and *n*-butylbenzene, a complete *n*-heptane sub-mechanism, abstraction reaction rate constants for the secondary benzyl hydrogen by $\dot{H}$, $\dot{O}H$, $H\dot{O}_2$, $\dot{C}H_3$, and $CH_3\dot{O}$ radicals and O_2 which were assigned to match the rates adopted in the base chemistry for abstraction reactions on secondary allylic hydrogens [9] and updated low temperature reaction pathways to correctly predict ignition delay times for the lower temperature experiments studied here. A full description of all modifications to the mechanism can be found in our previous publications [9, 11, 13, 14, 65].

RCM experiments were simulated using CHEMKIN-Pro [73]. For the ignition calculations in an RCM, the calculation uses a volume profile generated from the non-reactive pressure trace. The volume history used for the simulation is representative of the compression stroke and heat losses after the end of compression, which is an approach described by Mittal *et al.* [74]. All non-reactive pressure traces are available as Supplementary Material.

HPST simulations were also carried out using CHEMKIN-Pro, with the initial conditions of reflected shock temperature and pressure were used assuming constant volume conditions. The 3% / ms increase in pressure witnessed in the

experiments was simulated in a similar manner to the rapid compression machine simulations where a volume profile was generated to account for this pressure increase. We observed very little variation between predicted ignition delay times using (i) adiabatic, constant volume simulations, and (ii) including the 3% / ms pressure rise due to the relatively short ($\leq$ 2 ms) measurement times of these experiments. It is important to account for these facility effects for longer ignition times but as the experimental data obtained in this study are within this range adiabatic simulations suffice.

3.2. n-Decylbenzene surrogate results

The results obtained for the oxidation of the surrogates for n-decylbenzene are described below. Initially the data for n-propylbenzene / n-heptane will be described followed by the n-butylbenzene / n-heptane data and finally a comparison of the two surrogates will be shown. A complete glossary of all the shortened species names required for CHEMKIN-Pro and all experimental data can be found in the Supplementary Material.

3.2.1. n-Propylbenzene / n-Heptane mixtures

At all conditions studied experimental data was compared to simulations carried out using the detailed chemical kinetic mechanism described above using CHEMKIN-Pro [73] assuming adiabatic, constant volume conditions with no inhomogeneities for the shock tube experiments. Rapid compression machine experiments were simulated by taking non-reactive pressure traces and simulating taking these as the standard pressure (accounting for the pressure loss as a result

16

of heat as a result of the longer ignition delay times). Figures 2 and 3 show experimental data obtained in both the high pressure shock tube (filled symbols) and rapid compression machine (open symbols). Lines on the graphs relate to chemical kinetic mechanism simulations and it is clear that for both instruments the experimental data and simulations show reasonable agreement.
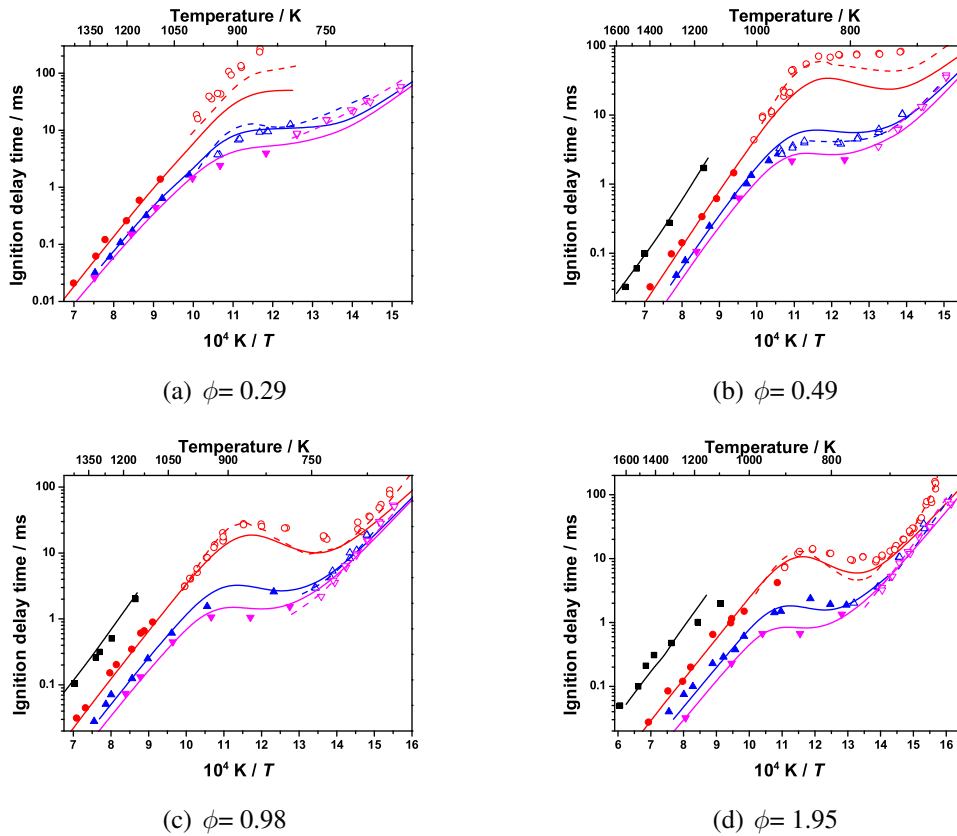
Influence of pressure on ignition delay time

(a) $\phi = 0.29$ (b) $\phi = 0.49$

(c) $\phi = 0.98$ (d) $\phi = 1.95$

Figure 2: Influence of varying reflected shock pressure on the reactivity of mixtures of *n*-propylbenzene and *n*-heptane; ■ – 1 atm, ● – 10 atm, ▲ – 30 atm, ▼ – 50 atm. Lines are model simulations; —— adiabatic simulation, – – – simulation including facility effects.

The influence of pressure for the *n*-propylbenzene / *n*-heptane mixtures is that an increase in pressure relates to a decrease in ignition delay times which relates to an increase in reactivity. At 900 K the extent of the variation of the reactivities is very consistent in that the difference in reactivity between 10 and 30 atm experiments is approximately a factor of 10 while the difference in reactivity between 30 and 50 is approximately a factor of 2, Fig. 2. Of course this results in 1 atm experiments taking the longest to ignite while 50 atm experiments have the shortest ignition delay times. Interestingly these experiments show some NTC behavior in particular at stoichiometric and rich conditions which were not observed for pure *n*-propylbenzene experiments [11]. This is attributed to the enhanced low temperature chemistry which occurs as an effect of the longer alkyl chain due to the *n*-heptane. This longer alkyl chain has additional CH_2 groups that allow the occurrence of fast $R\dot{O}_2$ isomerizations through six-membered ring transition states that lead to chain branching.

18

Influence of equivalence ratio on ignition delay time

The effect of equivalence ratio on ignition delay times was determined at 1, 10, 30 and 50 atm, Fig. 3. The effect of equivalence ratio at pressures of 1 atm at the four equivalence ratios studied (0.29, 0.48, 0.96 and 1.92) is shown in Fig. 3(a). At high temperatures, the fuel-lean mixtures react fastest and the fuel-rich slowest. As the temperature is lowered, the ignition times at different equivalence ratios converge. This behavior is captured by model simulations.

(a) 1 atm

(b) 10 atm

(c) 30 atm

(d) 50 atm
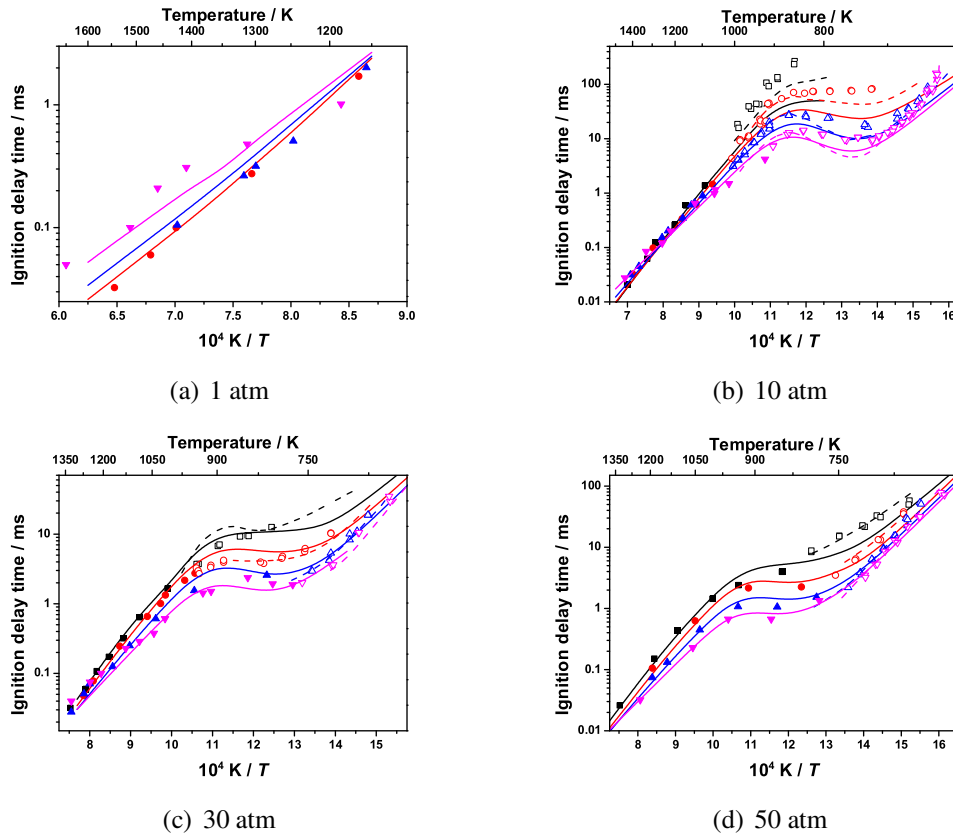
Figure 3: Influence of varying equivalence ratio (ϕ) on the reactivity of mixtures of *n*-propylbenzene and *n*-heptane; ■ – ϕ = 0.29, ● – ϕ = 0.49, ▲ – ϕ = 0.98, ▼ – ϕ = 1.95. Lines are model simulations; —— adiabatic simulation, – – – simulation including facility effects.

At low- and intermediate-temperatures fuel-rich mixtures ignite faster than fuel-lean ones. This behavior at intermediate temperatures is attributed to the chain branching sequence $RH + H\dot{O}_2 = \dot{R} + H_2O_2$ followed by $H_2O_2 (+ M) = \dot{O}H + \dot{O}H (+ M)$, where RH is the fuel components. In the present experiments, the equivalence ratio is increased by increasing the fuel concentration ([RH]) which enhances the rate of this branching sequence that produces two reactive $\dot{O}H$ radicals [65]. This effect is also seen at 30 and 50 atm, Fig 3(c) – 3(d). At low temperatures the reactivity is dominated by the addition of a fuel radical to molecular oxygen and subsequent low temperature chain branching reactions. Once again with the oxygen concentration remaining relatively constant in these experiments, it is the concentration of fuel radicals present which controls the rate of this sequence which results in fuel-rich mixtures igniting faster. Interestingly, NTC behavior is observed for most conditions which was not the case for pure *n*-propylbenzene. Again we believe this is due to the addition of *n*-heptane extending the length of the alkyl chain.

It can be seen that at high temperatures the influence of equivalence ratio on the reactivity of these mixtures is reduced, which is represented by their relatively similar ignition delay times when compared with the lower temperatures.

This behavior is replicated in the 30 and 50 atm data, Figs. 3(c) and 3(d), although the convergence of data in the 50 atm experiments cannot be seen within the restrictions of this study but judging by the relative slopes of the data and using the model simulations as a guide it is expected that at even higher temperatures, convergence and then crossover in reactivity will occur. The cross-over of ignition

20

delays of different equivalence ratios is due to the promoting effect of the fuel at low temperature due to the fuel + $H\dot{O}_2$ reaction and the fuel's inhibiting effect at high temperature due to its consumption of $\dot{H}$ atoms which reduces $\dot{H} + O_2$ chain branching.

3.3. Comparison of n-Propylbenzene, n-Propylbenzene / n-Heptane mixture and n-Heptane Oxidation

Experiments were carried out at $\phi \approx 1.0$ and 10 atm for the following mixtures, Fig. 4:

1. *n*-propylbenzene; black symbols and lines
2. *n*-propylbenzene / *n*-heptane; red symbols and lines
3. *n*-heptane; blue symbols and lines
4. *n*-heptane literature data [24, 32, 33, 35]; magenta symbols

These experiments were carried out in order to test the magnitude of the influence of the addition of *n*-heptane on the reactivity of the fuel. The least reactive mixture is *n*-propylbenzene, followed by the *n*-propylbenzene / *n*-heptane mixture and the most reactive is *n*-heptane, Fig. 4.

The main temperature range where there is a large discrepancy between the reactivities of each fuel mixture is in the low-temperature regime. Here the reactivity of the *n*-propylbenzene / *n*-heptane mixture is dependent upon both of the fuels. The mixture reacts faster than for pure *n*-propylbenzene due to the extended alkyl chain present as a result of the addition of *n*-heptane. Additionally the benzene ring acts as a radical sink causing a decrease in reactivity when compared
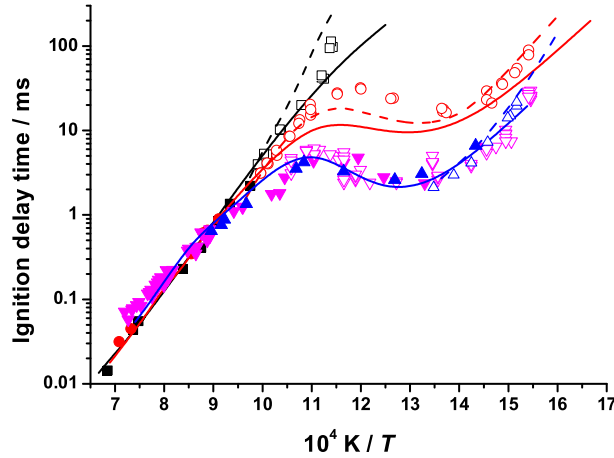
21

Figure 4: Three fuel comparison at $\phi \approx 1.0$ and 10 atm. ■ – *n*-propylbenzene data, ● – *n*-propylbenzene / *n*-heptane data, ▲ – *n*-heptane, ▼ – *n*-heptane literature data [24, 32, 33, 35]. Solid symbols represent shock tube data, open symbols depict RCM data. Lines are model simulations; —— adiabatic simulation, – – – simulation including facility effects.

to pure *n*-heptane. This indicates that the chemistry of *n*-heptane dominates the reactivity at these low- to intermediate-temperatures while the only effect of *n*-propylbenzene is to inhibit the *n*-heptane chemistry by competing with *n*-heptane for radicals required to initiate reactivity. This behavior was previously discussed by Herzler *et al.* [16] in a an ignition delay study of a mixture of 65% toluene and 35% *n*-heptane. When this data was compared to that of pure *n*-heptane reduced NTC reactivity was observed. This observation was further strengthened in the study of Hartmann *et al.* [18] who observed a significant reduction in reactivity in the NTC region when toluene was added to *n*-heptane mixture at a level of 40% toluene.

Interactions between the two fuel molecules did not appear as being important at high-temperatures as *n*-heptyl radicals are promptly consumed by β-scission reactions, without forming significant amounts of long lasting intermediates that can interact with the propylbenzene chemistry. On the other end, the resonantly stabilized 1-phenyl-1-propyl radical does not inhibit *n*-heptane reactivity at high temperature. At the higher temperatures studied here all three mixtures have similar reactivities shown by their similar ignition delay times in this range.

To further support these conclusions a brute force sensitivity analysis of different reaction rate constants was performed at 650 and 900 K, at 10 atm pressure and at $\phi = 0.98$, Figs. 5 and 6 using CHEMKIN-Pro [73]. The analyses were performed by increasing and decreasing both the forward and reverse rate constants by a factor of two, with sensitivities expressed using the formula:

$$S = \frac{\ln(\tau_+/\tau_-)}{\ln(k_+/k_-)} = \frac{\ln(\tau_+/\tau_-)}{\ln(2/0.5)}$$

A positive sensitivity coefficient indicates an inhibiting reaction while a negative sensitivity coefficient indicates a reaction promoting reactivity. Discussion of the key reactions at 1000 and 1500 K have been described in a previous publication [65].

The sensitivity results are separated into two plots: Fig. 5 for the negative sensitivities that promote reactivity and Fig. 6 for the positive sensitivities that inhibit reactivity. We have classified the selected reactions into three groups for explanation: (A) reactions related to *n*-heptane oxidation; (B) reactions related
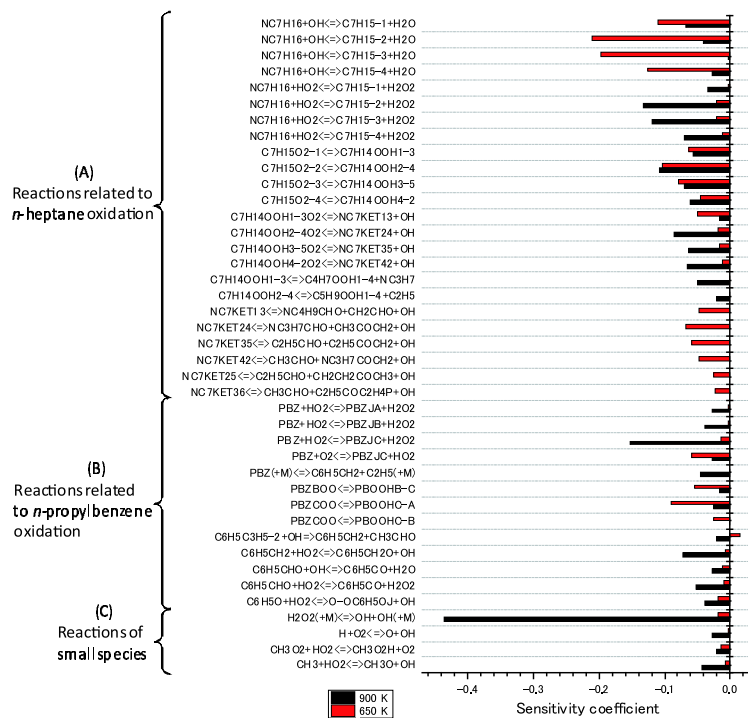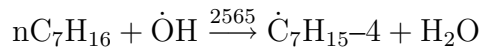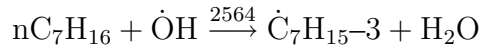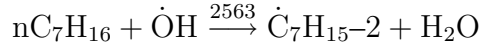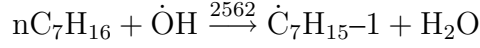
23

Figure 5: Sensitivity coefficients of main promoting reactions showing the effect of temperature at 650 and 900 K on n-propylbenzene / n-heptane ignition delay time, $\phi = 0.98$, $p_5 = 10$ atm.

to n-propylbenzene oxidation and (C) reactions of small species. A species naming dictionary can be found in the Supplementary Material of the online version of [11].

We begin our discussion with Fig. 5 which shows the negative sensitivities whose magnitudes are greater than 0.02. For group (A), most of the reactions show significant sensitivity coefficients at 650 and/or 900 K (typically with a magnitude of less than 0.04) and the number of the reactions showing high magnitude sensitivity coefficients is more than those of group (B) and (C). The H-atom abstraction reactions with $\dot{O}H$ radicals, $RH + \dot{O}H = \dot{R} + H_2O$, show the highest

24

magnitude sensitivity coefficients at 650 K in Fig. 5, significantly promoting the reactivity of the system.

$$nC_7H_{16} + \dot{O}H \xrightarrow{2562} \dot{C}_7H_{15}\text{--}1 + H_2O$$

$$nC_7H_{16} + \dot{O}H \xrightarrow{2563} \dot{C}_7H_{15}\text{--}2 + H_2O$$

$$nC_7H_{16} + \dot{O}H \xrightarrow{2564} \dot{C}_7H_{15}\text{--}3 + H_2O$$

$$nC_7H_{16} + \dot{O}H \xrightarrow{2565} \dot{C}_7H_{15}\text{--}4 + H_2O$$

The H-atom abstraction reactions with $H\dot{O}_2$ radicals, $RH + H\dot{O}_2 = \dot{R} + H_2O_2$, promote reactivity at 900 K while they do not promote reactivity as significantly at 650 K. The intra-molecular H-atom isomerization reactions, $R\dot{O}_2 \rightleftharpoons \dot{Q}OOH$, promote reactivity at both 650 and 900 K. The formation reactions of ketohydroperoxide species, $\dot{O}_2QOOH \rightleftharpoons$ ketohydroperoxide $+ \dot{O}H$, promote reactivity at 900 K but but show very little sensitivity at 650 K. The ketohydroperoxide decomposition reactions promote reactivity at 650 K while they show no sensitivity at 900 K. These results are consistent with the fact that at low temperature (650 K) the decomposition of the carbonyl hydroperoxide species represent a rate limiting limiting step in the low temperature degenerate branching process while at 900 K, where the hydroperoxyl group decomposes at a much faster rate, the competition between isomerizations and the propagation steps controls the $\dot{O}H$ production rate.

For group (B), on the other hand, the number of reactions showing significant sensitivity coefficients is less than for Group (A). The abstraction reaction of an alpha-site hydrogen atom on the alkyl chain of *n*-propylbenzene shows the largest negative sensitivity coefficient at 900 K in group (B). The fuel decomposition

25

reaction, PBZ(+M) = $C_6H_5\dot{C}H_2 + \dot{C}_2H_5$(+M), shows a significant sensitivity co-efficient at 900 K. The benzyl radical produced is subsequently converted to ben-zoxyl radical via the reaction of a benzyl and an hydroperoxyl radical ($C_6H_5\dot{C}H_2 + H\dot{O}_2 = C_6H_5CH_2\dot{O} + \dot{O}H$), and this reaction also shows an important sensitivity coefficient at 900 K. Intra-molecular H-atom isomerization reactions promote re-activity at 650 K. For group (C), the hydrogen peroxide decomposition reaction, H_2O_2(+M)= $\dot{O}H + \dot{O}H$ +(M), shows the highest sensitivity coefficient at 900 K, Fig. 5, significantly promoting reactivity.

$$H_2O_2(+M) \xrightarrow{50} \dot{O}H + \dot{O}H(+M)$$
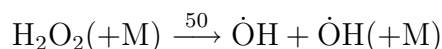
Results for the negative sensitivities show that the overall reactivity is mainly promoted by *n*-heptane oxidation reactions at both 650 and 900 K. In addition to that, the H_2O_2 decomposition reaction promotes reactivity at 900 K.

Figure 6 shows positive sensitivity coefficients greater than +0.02 and their reactions. Again, we have classified the selected reactions into the three groups for explanation. For group (A), many reactions inhibit reactivity at 650 and/or 900 K, but the magnitude of these sensitivity coefficients are not as high (typically less than 0.04) as their negative counterparts in Fig. 5. For group (B), on the other hand, the H-atom abstraction reactions with $\dot{O}H$ radicals show very high sensitivity coefficients at 650 K and inhibit reactivity significantly.

The H-atom abstraction reaction with $\dot{O}H$ radicals from *n*-propylbenzene show positive sensitivity coefficients, while those from *n*-heptane show negative sensi-tivity coefficients (Fig. 5). The reaction of $\dot{O}H$ radical at the alpha site on n-
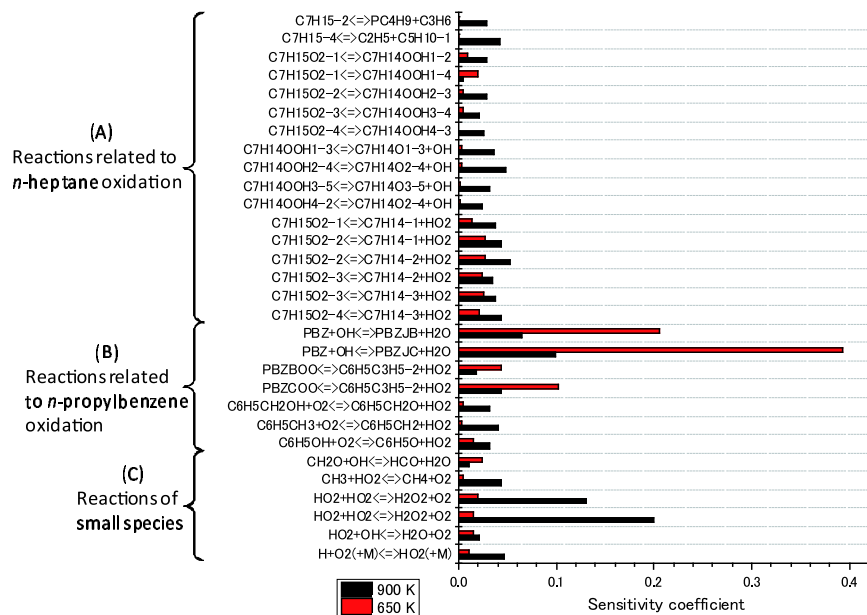
Figure 6: Sensitivity coefficients of main inhibiting reactions showing the effect of temperature at 650 and 900 K on n-propylbenzene / n-heptane ignition delay time, $\phi = 0.98$, $p_5 = 10$ atm.

propylbenzene is particularly inhibiting due to the formation of the un-reactive resonantly-stabilized alpha radical, PBZJC. For group (C), the duplicate reactions $H\dot{O}_2 + H\dot{O}_2 = H_2O_2 + O_2$ show very high sensitivity coefficients at 900 K. These termination reactions compete with the abstraction reactions on the fuel forming H_2O_2 which decomposes to two $\dot{O}H$ radicals, which is a source of branching at 900 K. From these results, the overall reactivity is mainly inhibited by the H-atom abstraction reaction with $\dot{O}H$ radical from n-propylbenzene at 650 K and the termination reactions involving $H\dot{O}_2$ radicals at 900 K.

3.3.1. n-Butylbenzene / n-heptane

Influence of pressure on ignition delay time

27

As is the case with the mixtures of *n*-propylbenzene and *n*-heptane, the influence of pressure for the *n*-butylbenzene / *n*-heptane mixtures shows that an increase in pressure results in a decrease in ignition delay times (i.e. an increase in reactivity), Fig. 7. Once again this results in 1 atm experiments in the shock tube taking the longest to ignite while 50 atm experiments have the shortest ignition delay times. NTC behavior is observed at $\phi = 0.5$, 1.0 and 2.0. At 900 K, the extent of the variation of the reactivities is very consistent with the results for the *n*-propylbenzene mixtures, in that the difference in reactivity between 10 and 30 atm experiments is approximately a factor of 10 while the difference in reactivity between 30 and 50 is approximately a factor of 2.

Influence of equivalence ratio on ignition delay time

The effect of equivalence ratio on ignition delay times is shown in Fig. 8. It is clear that at low- and intermediate-temperatures fuel-rich mixtures ignite faster than fuel-lean ones 8(b). As discussed previously for the mixtures of *n*-propylbenzene / *n*-heptane this behavior at intermediate temperatures (around 900 K) is attributed to the chain branching sequence $RH + H\dot{O}_2 = \dot{R} + H_2O_2$ followed by $H_2O_2 (+ M) = \dot{O}H + \dot{O}H (+ M)$, where RH is the fuel components. In the present experiments, the equivalence ratio is increased by increasing the fuel concentration ([RH]) which enhances the rate of this branching sequence that produces two reactive $\dot{O}H$ radicals [65]. This effect is also seen at 30 and 50 atm, Figs. 8(c)–8(d). At low temperature (around 650 K), the reactivity is dominated by the addition of a fuel radical to molecular oxygen the subsequent low temperature chain branching reactions. Once again with the oxygen concentration
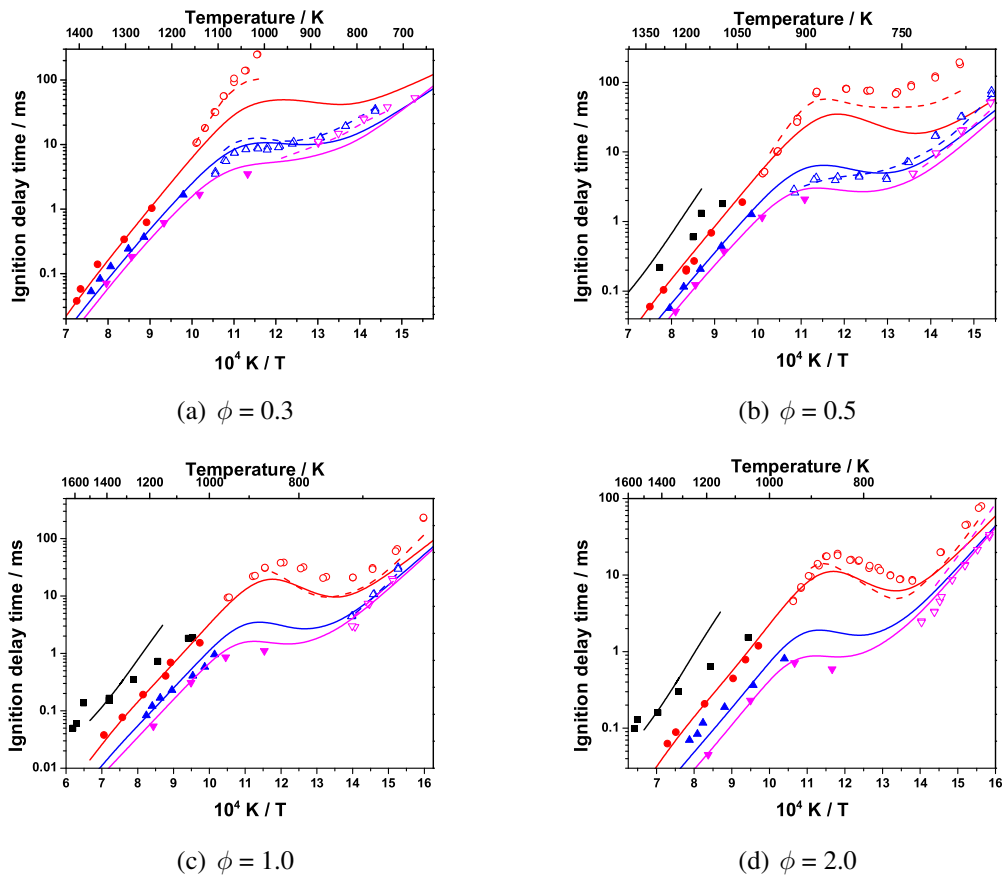
Figure 7: Influence of varying reflected shock pressure on the reactivity of mixtures of *n*-butylbenzene and *n*-heptane; ■ – 1 atm, ● – 10 atm, ▲ – 30 atm, ▼ – 50 atm. Lines are model simulations; —— adiabatic simulation, – – – simulation including facility effects.

remaining relatively constant in these experiments, it is the concentration of fuel radicals present which controls the rate of this sequence which results in fuel-rich mixtures igniting faster. Interestingly, NTC behavior is observed for most conditions which was not the case for pure *n*-propylbenzene. Again we believe this is due to the addition of *n*-heptane extending the effective length of the alkyl chain in the mixture.
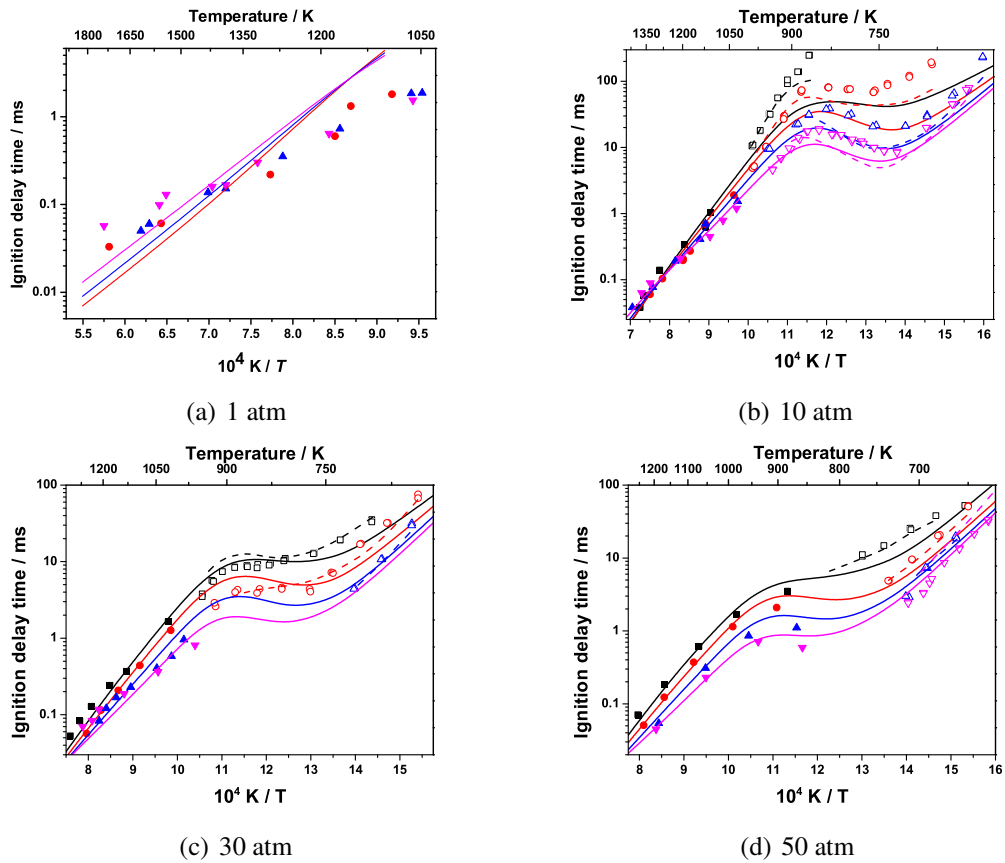
(a) 1 atm (b) 10 atm

(c) 30 atm (d) 50 atm

Figure 8: Influence of varying equivalence ratio (ϕ) on the reactivity of mixtures of n-butylbenzene and n-heptane; ■ – $\phi = 0.3$, ● – $\phi = 0.5$, ▲ – $\phi = 1.0$, ▼ – $\phi = 2.0$. Lines are model simulations; —— adiabatic simulation, – – – simulation including facility effects.

It can be seen that at high temperatures the influence of equivalence ratio on the ignition delay time of these mixtures is reduced compared with the lower temperatures. This change in behavior at high temperature is due to the lessening influence of the fuel + $H\dot{O}_2$ radical reaction whose influence on the sensitivity of ignition delay to equivalence ratio was discussed earlier. This reduction in the effect of equivalence ratio at high temperature is replicated by the 30 and 50 atm

30

data, Figs. 8(c)–8(d), although once again the the convergence of data in the 50 atm experiments can not be seen within the restrictions of this study but judging by the relative slopes of the data and using the model simulations as a guide it is expected that at even higher temperatures that convergence and then crossover in reactivity will occur.

4. Comparison of mixtures using various *n*-alkylbenzenes

4.1. n-Propylbenzene and n-butylbenzene / n-heptane mixture comparisons

All ignition delay data discussed above was compared and a series of trends have been outlined. Data comparing the oxidation of mixtures of *n*-propylbenzene / *n*-heptane and *n*-butylbenzene / *n*-heptane is shown in Figs. 9–11.

From this data it was noted that both mixtures showed similar ignition delay times which indicate similar level of reactivity. The reaction mechanism described previously was used to simulate this data and shows reasonable agreement with all data sets. It is expected that the agreement of ignition delay times is due to the reactivity of the mixture being largely controlled by the *n*-heptane component while the alkylbenzene component only works to inhibit the reactivity and this occurs to the same extent for both mixtures. Also note that the n-heptane component was greater in the n-propylbenzene mixture than in the n-butylbenzene mixture in order to match the C/H ratio in the target fuel *n*-decylbenzene. The higher amount of *n*-heptane in the *n*-propylbenzene mixture help to compensate for *n*-propylbenzene's shorter alkyl chain.
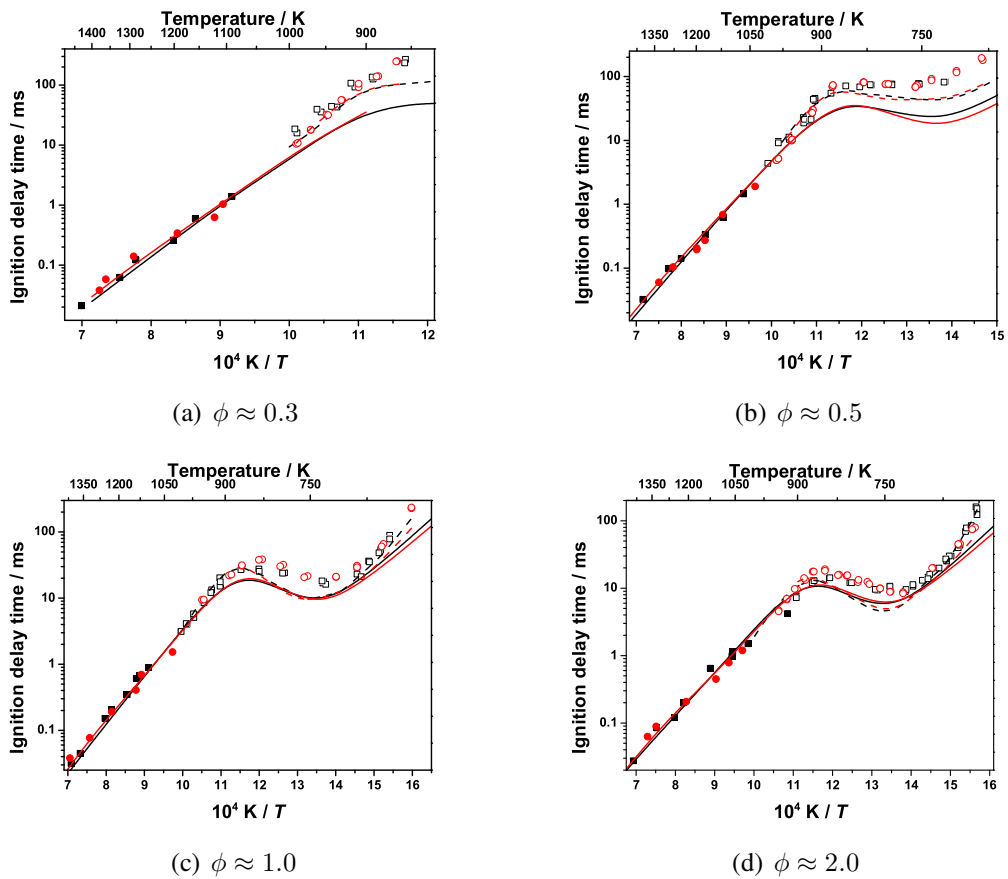
31

(a) $\phi \approx 0.3$

(b) $\phi \approx 0.5$

(c) $\phi \approx 1.0$

(d) $\phi \approx 2.0$

Figure 9: A comparison of *n*-propylbenzene / *n*-heptane mixtures and *n*-butylbenzene / *n*-heptane mixtures at various equivalence ratios (ϕ) and at 10 atm. ■ – *n*-propylbenzene data, ● – *n*-butylbenzene data. Solid symbols: Shock tube, Open symbols: RCM. Lines are model simulations; —— adiabatic simulation, – – – simulation including facility effects.

4.2. Ethylbenzene / n-heptane mixture comparison with other surrogates

To confirm the effect of alkyl chain length of alkylbenzenes on ignition delay times, it was decided to investigate the oxidation of an ethylbenzene / *n*-heptane mixture and compare the experimental data to those previously recorded for the other two *n*-decylbenzene surrogates. A 48% / 52% mixture of ethylbenzene and *n*-heptane was used. Experiments were carried out in both the shock tube and
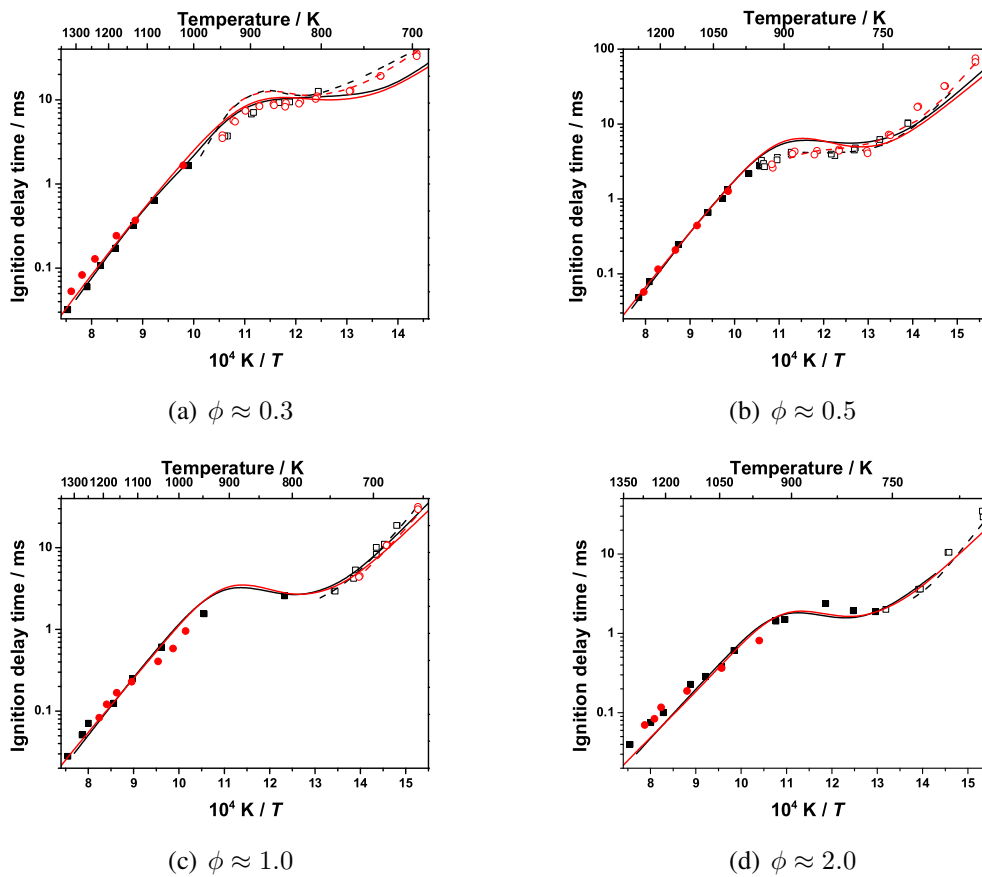
(a) $\phi \approx 0.3$

(b) $\phi \approx 0.5$

(c) $\phi \approx 1.0$

(d) $\phi \approx 2.0$

Figure 10: A comparison of *n*-propylbenzene / *n*-heptane mixtures and *n*-butylbenzene / *n*-heptane mixtures at various equivalence ratios (ϕ) and at 30 atm. ■ – *n*-propylbenzene data, ● – *n*-butylbenzene data. Solid symbols: Shock tube, Open symbols: RCM. Lines are model simulations; —— adiabatic simulation, – – – simulation including facility effects.

RCM over the full temperature range at and equivalence ratio of 2.0 and at a pressure of 10 atm. Figure 12 shows the comparison of the three fuel mixtures

As can be seen from this figure all mixtures show similar reactivity throughout the temperature range including in the NTC region. The trends in the data are captured quite well by the model simulations while there is some discrepancy between experimental data and all model simulations in the NTC range. While
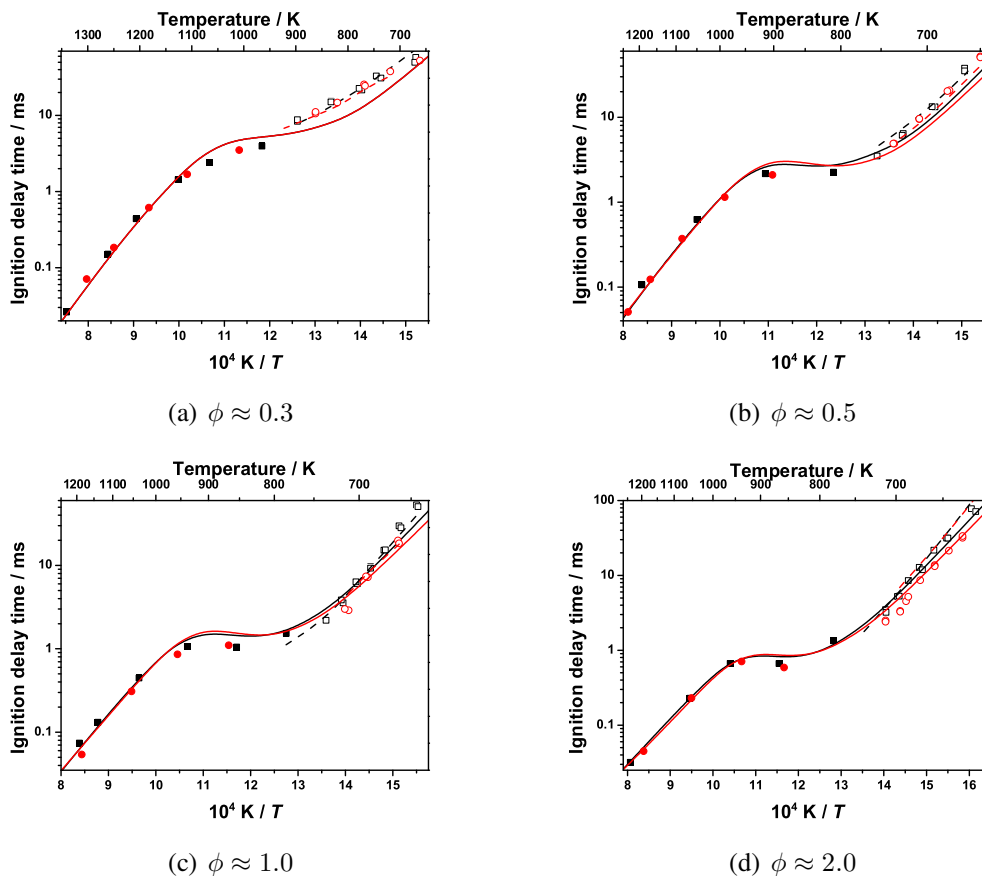
Figure 11: A comparison of *n*-propylbenzene / *n*-heptane mixtures and *n*-butylbenzene / *n*-heptane mixtures at various equivalence ratios (ϕ) and at 50 atm. ■ – *n*-propylbenzene data, ● – *n*-butylbenzene data. Solid symbols: Shock tube, Open symbols: RCM. Lines are model simulations; —— adiabatic simulation, – – – simulation including facility effects.

we only are examining homogeneous ignition and this is not a comprehensive study, it leads us to believe that a carefully chosen surrogate can resolve some of the difficulties involved in using large alkylbenzenes, in particular the problem of vapor pressure.
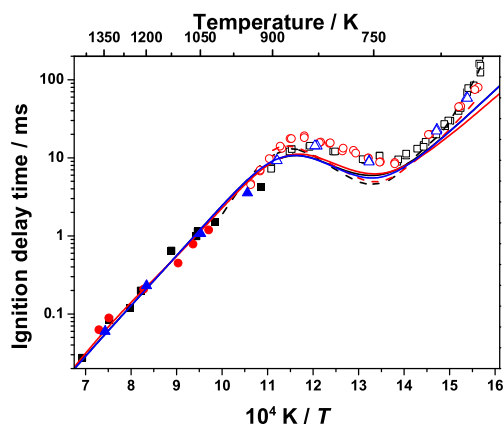
Figure 12: A comparison of *n*-propylbenzene / *n*-heptane mixtures and *n*-butylbenzene / *n*-heptane mixtures at ϕ = 2.0 and at 10 atm pressure. ■ – *n*-propylbenzene / *n*-heptane data, ● – *n*-butylbenzene / *n*-heptane data, ▲ – ethylbenzene / *n*-heptane data. Solid symbols represent shock tube data, open symbols depict RCM data. Lines are model simulations; —— adiabatic simulation, – – – simulation including facility effects.

5. Conclusions

This paper represents the first experimental study of the ignition of two surrogates for the large alkylbenzene class of compounds contained in diesel fuels, namely *n*-decylbenzene over a wide range of temperatures and pressures. A 57% *n*-propylbenzene / 43% *n*-heptane in air mixture was used along with a 64% *n*-butylbenzene / 36% *n*-heptane in air mixtures. These mixtures were selected to contain a similar hydrogen:carbon ratio (1.685 and 1.65, respectively) and similar aromatic versus alkane chain content when compared to *n*-decylbenzene whose hydrogen:carbon ratio is 1.625.

Equivalence ratios of 0.3, 0.5, 1.0 and 2.0 were studied for *n*-propylbenzene / *n*-heptane and *n*-butylbenzene / *n*-heptane mixtures. For both mixtures compressed pressures of 1, 10, 30 and 50 atm were measured in both a shock tube and

rapid compression machine at NUI Galway. The temperature range studied was from approximately 650–1700 K.

The effects of reflected shock pressure and equivalence ratio on ignition delay time were determined and common trends highlighted. For both mixtures it was found that an increase in reflected shock pressure resulted in shorter ignition delay times (that is higher reactivity) for all equivalence ratios investigated, which is typical of the influence of pressure on fuel reactivity. The effect of equivalence ratio is as expected in that fuel-rich mixtures have shorter ignition delay times indicating higher reactivity than fuel-lean mixtures throughout the range although at higher temperatures the reactivity begins to converge. This convergence was noted in particular for the 10 atm experiments while at 30 and 50 atm it is expected that this will occur at even higher temperatures than those available in this study. This indicates that there is still some low and intermediate temperature chemistry occurring even at these elevated temperatures This behavior has been observed for the pure *n*-propylbenzene and pure *n*-butylbenzene experiments studied in our previous publications.

When comparing pure *n*-propylbenzene and pure *n*-heptane to the mixture of *n*-propylbenzene and *n*-heptane it was noted in the low temperature regime there is a large discrepancy between the reactivities of each fuel. The mixture reacts faster than pure *n*-propylbenzene due to the fraction of alkyl chain present in the mixture been increased due to the addition of *n*-heptane. Additionally the resonantly stabilized alpha radical produced by the *n*-propylbenzene acts as a radical sink causing a decrease in reactivity when compared to pure *n*-heptane. This in-

36

dicates that the chemistry of *n*-heptane dominates the reactivity at these low- to intermediate-temperatures while the only effect of *n*-propylbenzene is to inhibit the *n*-heptane chemistry by competing with *n*-heptane for radicals required to initiate reactivity. These conclusions are consistent with previous literature studies.

In the comparison between the *n*-propylbenzene / *n*-heptane mixtures with *n*-butylbenzene / *n*-heptane mixtures there was no discernible difference between the reactivity of the two surrogates for *n*-decylbenzene. These similar results were encouraging as they indicate that both mixtures are surrogates that accurately represent the homogeneous ignition of *n*-decylbenzene, representing a large alkylbenzene. Criteria other than ignition behavior can be used to select which surrogate mixture best matches *n*-decylbenzene. Another criterion is matching the physical behavior of diesel fuel, including molecular weight, boiling point, and density. In this case, the surrogate containing *n*-butylbenzene would be best because its carbon number of C10 is most representative of the carbon number range of alkylbenzenes in diesel fuel (C9 to C20) [3]. Additionally as the vapor pressure of *n*-butylbenzene made these experiments very difficult, a study was carried out using a mixture of ethylbenzene and *n*-heptane and ignition delay times measured compared well with those of both *n*-propylbenzene / *n*-heptane and *n*-butylbenzene / *n*-heptane mixtures indicating that this could also be used as the surrogate for the large alkylbenzene while avoiding vapor pressure issues.

A reaction mechanism published previously was used to simulate this data. Overall the reaction mechanism captures the experimental data reasonably well.

37

6. Acknowledgments

References

[1] J. T. Farrell, N. P. Cernansky, F. L. Dryer, D. G. Friend, C. A. Hergart, C. K. Law, R. M. McDavid, C. J. Mueller, A. K. Patel, H. Pitsch, SAE Technical Paper, 2007-01-0201 (2007).

[2] W. J. Pitz, C. J. Mueller, Prog. Energy Combust. Sci. 37 (2011) 330–350.

[3] C. J. Mueller, W. J. Cannella, T. J. Bruno, B. Bunting, H. D. Dettman, J. A. Franz, M. L. Huber, M. Natarajan, W. J. Pitz, M. A. Ratcliff, K. Wright, Energy Fuels 26(6) (2012) 3284–3303.

[4] T. Litzinger, K. Brezinsky, I. Glassman, Combust. Sci. Technol. 50 (1996) 117–133.

[5] A. Roubaud, R. Minetti, L. R. Sochet, Combust. Flame 121 (2000) 535–541.

[6] A. Roubaud, O. Lemaire, R. Minetti, L. R. Sochet, Combust. Flame 123 (2000) 561–571.

[7] P. Dagaut, A. Ristori, A. El Bakali, M. Cathonnet, Fuel 81 (2002) 173–184.

[8] S. Gudiyella, K. Brezinsky, Combust. Flame 159 (2012) 940–958.

[9] D. Darcy, C. J. Tobin, K. Yasunaga, J. M. Simmie, J. Würmel, T. Niass, O. Mathieu, S. S. Ahmed, C. K. Westbrook, H. J. Curran, Combust. Flame 159 (2012) 2219–2232.

[10] P. Diévart, P. Dagaut, Proc. Combust. Inst. 33 (2011) 209–216.

[11] D. Darcy, H. Nakamura, M. Mehl, C. Tobin, W. K. Metcalfe, W. J. Pitz, C. K. Westbrook, H. J. Curran, Combust. Flame (2013) http://dx.doi.org/10.1016/j.combustflame.2013.08.001.

[12] M. Ribaucour, A. Roubaud, R. Minetti, L. R. Sochet, Proc. Combust. Inst. 28 (2000) 1701–1707.

[13] B. Husson, R. Bounaceur, K. Tanaka, M. Ferrari, O. Herbinet, P. A. Glaude, R. Fournet, F. Battin-Leclerc, M. Crochet, G. Vanhove, R. Minetti, C. J. Tobin, K. Yasunaga, J. M. Simmie, H. J. Curran, T. Niass, O. Mathieu, S. S. Ahmed, Combust. Flame 159 (2012) 1399–1416.

[14] H. Nakamura, D. Darcy, M. Mehl, C. Tobin, W. K. Metcalfe, W. J. Pitz, C. K. Westbrook, H. J. Curran, Combust. Flame (2013) http://dx.doi.org/10.1016/j.combustflame.2013.08.002.

[15] J. Andrae, D. Johansson, P. Björnbom, P. Risberg, G.T. Kalghatgi, Combust. Flame 140 (2005) 267–286.

[16] J. Herzler, M. Fikri, K. Hitzbleck, R. Starke, C. Schulz, P. Roth, G. T. Kalghatgi, Combust. Flame 149 (2007) 25–31.

[17] R. Minetti, M. Carlier, M. Ribacour, E. Therssen, L. R. Sochet, Combust. Flame 102 (1995) 298–309.

[18] M. Hartmann, I. Gushterova, M. Fikiri, C. Schulz, R. Schießl, U. Mass, Combust. Flame 158 (2011) 172–178.

[19] D.S. Kim, C.S. Lee, Fuel 85 (2006) 695–704.

[20] S. Tanaka, F. Ayala, J. C. Keck, J. B. Heywood, Combust. Flame 132 (2003) 219–239.

[21] X. C. Lu, W. Chen, Z. Huang, Fuel 84 (2005) 1074–1083.

[22] X. C. Lu, W. Chen, Z. Huang, Fuel 84 (2005) 1084–1092.

[23] J. P. Szybist, A. L. Boehman, D. C. Haworth, H. Koga, Combust. Flame 149 (2007) 112–128.

[24] H. K. Ciezki, G. Adomeit, Combust. Flame 93 (1993) 421–433.

[25] K. Fieweger, R. Blumenthal, G. Adomeit, Combust. Flame 109 (1997) 599–619.

[26] B. M. Gauthier, D. F. Davidson, R. K. Hanson, Combust. Flame 139 (2004) 300–311.

[27] M. B. Colket, III, L. J. Spadaccini, J. Prop. Power 17 (2001) 315–323.

[28] S. S. Vasu, D. F. Davidson, R. K. Hanson, Combust. Flame 156 (2009) 736–749.

[29] B. Akih-Kumgeh, J. M. Bergthorson, Energy Fuels 24 (2010) 2439–2448.

[30] D. F. Davidson, Z. Hong, G. L. Pilla, A. Farooq, R. D. Cook, R. K. Hanson, Combust. Flame 157 (2010) 1899–1905.

[31] D. F. Davidson, D. C. Horning, R. K. Hanson, B. Hitch, 22nd Int. Symp. Shock Waves (1999) paper 360.

[32] D. C. Horning, D. F. Davidson, R. K. Hanson, J. Prop. Power 18 (2002) 363–371.

[33] K. A. Heufer, H. Olivier, Shock Waves 20/4 (2010) 307–316.

[34] J. F. Griffiths, P. A. Halford-Maw, D. J. Rose, Combust. Flame 95 (1993) 291–306.

[35] E. J. Silke, H. J. Curran, J. M. Simmie, Proc. Comb. Inst. 30 (2005) 2639–2647.

[36] A. Chakir, M. Bellimam, J. C. Boettner, M. Cathonnet, Int. J. Chem. Kinet. 24 (1992) 385–410.

[37] P. Dagaut, M. Reuillon, M. Cathonnet, Combust. Sci. Technol. 95 (1994) 233–260.

[38] P. Dagaut, M. Reuillon, M. Cathonnet, Combust. Flame 101 (1995) 132–140.

[39] O. Herbinet, B. Husson, Z. Serinyel, M. Cord, V. Warth, R. Fournet, P.-A. Glaude, B. Sirjean, F. Battin-Leclerc, Z. Wang, M. Xie, Z Cheng, F. Qi, Combust. Flame 159 (2012) 3455–3471.

[40] D. B. Lenhert, D. L. Miller, N. P. Cernansky, K. G. Owens, Combust. Flame 156 (2009) 549–564.

[41] P. Berta, S. K. Aggarwal, I. K. Puri, Combust. Flame 145 (2006) 740–764.

[42] A. T. Holley, Y. Dong, M. G. Andac, F. N. Egolfopoulos, Combust. Flame 144 (2006) 448–460.

[43] W. Liu, D. Zhu, N. Wu, C. K. Law, Combust. Flame 157 (2010) 259–266.

[44] C. Yao, C. Cheng, S. Liu, Z. Tian, J. Wang, Fuel 88 (2009) 1752–1757.

[45] A. J. Smallbone, W. Liu, C. K. Law, X. Q. You, H. Wang, Proc. Combust. Inst. 32 (2009) 1245–1252.

[46] C. M. Coats, A. Williams, Proc. Combust. Inst. 17 (1978) 611–621.

[47] C. K. Westbrook, J. Warnatz, W. J. Pitz, Proc. Combust. Inst. 22 (1988) 893–901.

[48] C. Chevalier, W. J. Pitz, J. Warnatz, C. K. Westbrook, H. Melenk, Proc. Combust. Inst. 24 (1992) 92–101.

[49] E. Ranzi, P. Gaffuri, T. Faravelli, P. Dagaut, Combust. Flame 103 (1995) 91–106.

[50] T. J. Held, A. J. Marchese, F. L. Dryer, Combust. Sci. Technol. 123 (1997) 107–146.

[51] H. J. Curran, P. Gaffuri, W. J. Pitz, C.K. Westbrook, Combust. Flame 114 (1998) 149–177.

[52] H. J. Curran, W. J. Pitz, C. K. Westbrook, C. V. Callahan, F. L. Dryer, Proc. Comb. Inst. 27 (1998) 379–387.

[53] M. Mehl, W. J. Pitz, C. K. Westbrook, H. J. Curran, Proc. Combust. Inst. 33 (2011) 193–200.

[54] D. M. A. Karwat, S. W. Wagnon, M. S. Wooldridge, C. K. Westbrook, Combust. Flame (2013) http://dx.doi.org/10.1016/j.combustflame.2013.06.029.

[55] G. T. Kalghatgi, R. A. Head, SAE Paper 2004-01-1969 (2004).

[56] J. C. G. Andrae, D. Johansson, P. Björnbom, P. Risberg, G. T. Kalghatgi, Combust. Flame 140 (2005) 267–286.

[57] J. C. G. Andrae, P. Björnbom, R. F. Cracknell, G.T. Kalghatgi, Combust. Flame 149 (2007) 2–24.

[58] J. C. G. Andrae, T. Brinck, G. T. Kalghatgi, Combust. Flame 155 (2008) 696–712.

[59] D. Bradley, R.A. Head, Combust. Flame 147 (2006) 171–184.

[60] A. Dubreuil, F. Foucher, C. Mounaïm-Rousselle, G. Dayma, P. Dagaut, Proc. Combust. Inst. 31 (2007) 2879–2886.

[61] H. Machrafi, S. Cavadias, P. Gilbert, Fuel Proc. Technol. 89 (2008) 1007–1016.

[62] S. Tanaka, F. Ayala, J. C. Keck, J. B. Heywood, Combust. Flame 132 (2003) 219–239.

[63] G. Vanhove, G. Petit, R. Minetti, Combust. Flame 145 (2006) 521–532.

[64] R. Di Sante, Combust. Flame 159 (2012) 55–63.

[65] D. Darcy, M. Mehl, J. M. Simmie, J. Würmel, W. K. Metcalfe, C. K. West-brook, W. J. Pitz, H. J. Curran, Proc. Combust. Inst. 34 (2013) 411–418.

[66] C. Morley, GasEq, Version 0.76, http//www.gaseq.co.uk (2004).

[67] W. S. Affleck, A. Thomas, Proc. Inst. Mech. Eng. 183 (1968–1969) 365–385.

[68] L. Brett, J. MacNamara, P. Musch, J. M. Simmie, Combust. Flame 124 (2001) 326–329.

[69] D. Lee, S. Hochgreb, Combust. Flame 114 (1998) 531–545.

[70] D. Lee, S. Hochgreb, Int. J. Chem. Kinet. 30 (1998) 385–406.

[71] J. Würmel, J. M. Simmie, H. J. Curran, Int. J. Vehicle Design 44 (2007) 84–106.

[72] R. Mével, P. A. Boettcher, J. E. Shepherd, Chem. Phys. Lett. 531 (2012) 22–27.

[73] CHEMKIN-Pro 15101, Reaction Design, San Diego, (2010).

[74] G. Mittal, C. J. Sung, M. Fairweather, A. S. Tomlin, J. F. Griffiths, K. J. Hughes, Proc. Combust. Inst. 31 (2007) 419–427.

[75] C. K. Westbrook, H. J. Curran, W. J. Pitz, J. F. Griffiths, C. Mohamed, S. K. Wo, Proc. Combust. Inst. 27 (1998) 371–378.